High frequency photoacoustic spectral analysis of erythrocyte programmed cell death (eryptosis)

Muhannad N. Fadhel, Eric M. Strohm and Michael C. Kolios*

Department of Physics, Ryerson University
Institute for Biomedical Engineering, Science and Technology (iBEST)
Keenan Research Centre for Biomedical Science of St. Michael's Hospital
Toronto, Ontario
mkolios@ryerson.ca

***Abstract*—Prior to hemolysis, erythrocytes undergo programmed cell death called eryptosis. Eryptosis is characterized by cell shrinkage, membrane blebbing and phosphatidylserine exposure. The high optical absorption of erythrocytes enables their photoacoustic (PA) detection and characterization. PA spectral analysis has been used to assess morphological changes of erythrocytes (e.g. size/shape). Normal and eryptotic RBCs (induced using sphingomyelinase (SMase)) were suspended on a substrate covered with 1% agarose. The PA signals of individual RBCs illuminated with a 532 nm laser were acquired using three ultrasound transducers with center frequencies of 200, 375 and 900 MHz. Frequency analysis of PA signals were applied to quantify the changes between normal and eryptotic RBCs. The results demonstrated significant changes in the spectral parameters. These parameters correlated to change in the RBC shape from the biconcave to spherical. This study also addressed examined the effects of ultrasound transducer focus on measured spectral parameters.**

Keywords: sphingomyelinase; eryptosis; photoacoustic spectral analysis; high frequency.

I. INTRODUCTION

Ceramide is a lipid chain molecule that has a significant contribution in signalling pathways. The pathways of ceramide activation range from inflammatory responses to cell migration and senescence [1]. Ceramide is present within the lipid bilayer at high concentrations and makes up one of the four common phospholipids found in the plasma membrane (sphingomyelin). The mechanism of ceramide signaling occurs in the plasma membrane through the activation of the enzyme sphingomyelinase (SMase) which hydrolyze the sphingomyelin into ceramide.

The role of ceramide for regulating cancer therapy has been studied [2]. A new class of cancer therapeutic drugs focuses on disrupting endothelial cells of tumour vasculatures [3]. There are significant advantages in targeting tumour vasculatures due to the genetic stability endothelial cells have over cancer cells [4]. Stress induction of endothelial cells have been shown to signal apoptosis in endothelial cells and increase SMase [5]. SMase is linked to secondary tumour cell death and therefore improves the efficacy of the cancer therapy [6], [7].

Photoacoustics (PA) has been proposed as an accessible and non-invasive imaging modality for monitoring tumours [8], [9]. PA can be used to detect changes to the cellular and molecular structures, which represents the new era for more accurate and early response assessment to therapy [10].

PA imaging has potentially high contrast due to the strong optical absorption of hemoglobin compared to the surrounding tissues at typical illumination wavelengths. PA imaging can provide information about the sate of red blood cells (RBCs), due to the high hemoglobin concentration inside RBCs, at a depth of several centimetres into the tissue [11]. Links between physical and biochemical changes of RBCs have been investigated and identified during cancer therapies, blood vessel disruption, and RBCs exposure to SMase [12]–[14]. The activation of the ceramide pathway causes the RBCs to undergo programmed cell death called eryptosis [13]. Eryptosis is associated with changes in the lipid membrane organization and loss in the biconcave shape of RBCs. The potential of PA imaging in detecting and quantifying eryptotic RBCs has not been investigated. In this paper, we examine and quantify the changes in PA signals due to SMase exposure to individual RBCs using high frequency ultrasound.

II. METHODS

A. Sample preparation

Blood samples were extracted from a healthy male volunteer through finger prick. This was done under Ryerson University Ethics protocol # 2015-203. The extracted blood was diluted in a vial with a dilution factor of 1:250, resulting in $2x10^4$ cells/µl, counted using a hemocytometer. The blood sample was diluted using Dulbecco's modified Eagle's Medial (DMEM) containing 10% fetal bovine serum (FBS). The media maintains the viability and sparsity of RBCs. To mimic RBCs in suspension, 2 ml of the diluted blood sample were deposited into a glass bottom petri dish (Mattek Corporation, USA) with 1 ml of 1% agarose (sigma Aldrich, CA) to minimize reflection from the sample holder [15]. The tested samples were normal biconcave RBCs and eryptotic RBCs. Eryptosis was induced by adding 50 mU/ml of SMase (sigma Aldrich, CA) to healthy RBCs for 5 minutes at 37ºC before signal acquisition. Optical images of the two samples were acquired using Olympus IX71 (Olympus, JP) with 40x objective lens (Fig. 1). PA signals were measured and analyzed at different ultrasound frequencies as discussed in the following sections.

B. *Experimental setup*

Changes in individual RBCs as a result of SMase exposure were examined using a PA microscope. It is composed of a high frequency ultrasound system (Kibero GmbH, DE), a short pulsed laser (Teem Photonics, FR) and Olympus IX81 optical microscope (Olympus, JP) enclosed in a temperature controlled chamber at 37ºC (Fig. 2) [16], [17]. A laser focused at 10 µm spot using 10x objective lens was used to interrogate individual RBCs. 532 nm laser pulsed at 4 kHz, pulse width of 330 ps, and linewidth of 10 nm was used. The generated PA signals were acquired using three ultrasound transducers with center frequencies of 200, 375 and 900 MHz and signals were average 200 times, to improve the SNR. 25 biconcave and 25 eryptotic RBCs were investigated using the three ultrasound transducers, resulting in a total of 150 radiofrequency (RF) signals. Signal analysis is discussed in the following section.

Fig. 1. Optical images at 400x magnification of normal biconcave RBCs (left) and eryptotic RBCs induced using SMase (right). The scale bar is 15 µm.

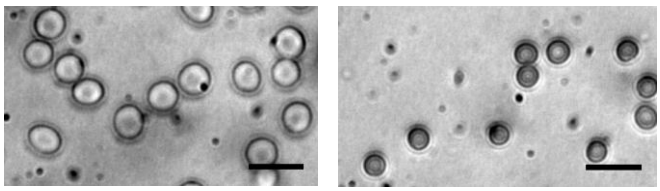

C. *Analysis of PA signals*

Frequency analysis of acquired RF signals was conducted to extract information not readily apparent in the time domain. The RF signals were time gated using a hanning window size of 25 ns. The calculated power spectra were normalized to a reference signal acquired from a 50 nm thick gold film for each transducer to reduce the transducer effect on the calculated parameters. The spectral slope, y-intercept, midband fit (MBF) were calculated from the power spectra for the 200 and 375 MHz transducers. Periodically occurring minima were identified for the 900 MHz transducer. These parameters were used to extract information about the morphology and hemoglobin content of individual RBCs to discriminate between biconcave and eryptotic RBCs.

Fig. 2. Schematic representation of the PA microscope system. The green shade represents laser intensity.

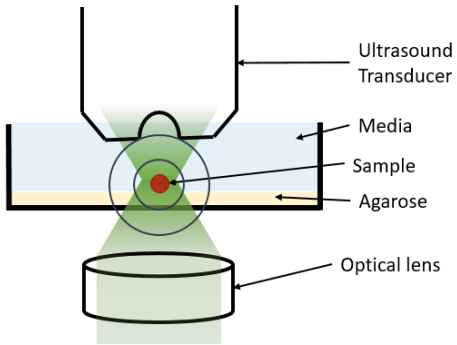

III. Results and Discussion

Optical images of the normal and SMase induced RBCs are presented in Fig. 1. The images demonstrate an observable change in shape from the normal biconcave to spherical as previously published in the literature [12]. SMase is a biological signal for stress which activates eryptosis [13]. Eryptosis is associated with the loss of band 3 protein function; band 3 protein is a transmembrane protein that acts in anchoring the cell lipid bilayer to its cytoskeleton. Loss in its function has been linked to shape changes of RBCs [18].

Representative RF signals measured using the three ultrasound transducers are presented in Fig. 3. The time domain signals suggest a similar number of cycles for both categories of RBCs and a decrease in the amplitude in the generated RF signals between normal and eryptotic RBCs for the 200 and 375 MHz transducers. For 900 MHz transducer, the number of cycles increased and amplitude decreased for eryptotic RBCs.

Frequency domain analysis of PA signals are presented in Fig. 4. Flat or sloped spectra were observed for all transducers in the case of normal RBCs. For the eryptotic RBCs and using the 200 and 375 MHz transducers, flat or sloped spectra were also observed, whereas spectral minima were observed when using the 900 MHz transducer for all examined cells. The spectral parameters for the 200 and 375 MHz transducer are presented in table 1. The results demonstrate significant increase in the y-intercept, and decrease in the spectral slope and MBF for both transducers. The decrease in the slope of eryptotic RBCs is linked to an increase in the apparent absorber size [19]; this is due to the increase in the thickness of the RBCs as they undergo shape change. An increase in the y-intercept is would typically be attributed to an increase in the concentration of absorbers (hemoglobin) [19]. However, the hemoglobin concentration in eryptotic RBCs is typically lower as hemoglobin molecules leak outside the cells [14]. The increase in the y-intercept is attributed to the change in the power spectra shapes that occur at higher frequencies, as seen in the analysis of the data using the 900 MHz transducer. The change in the spectral shapes increase the slope for the treated RBCs (which are outside of the quasi-linear regime), and therefore change the y-intercept values.

TABLE 1. Spectral parameters of the slope, y-intercept and MBF of normal and SMase induced RBCs. The blue and red colours represent data acquired using the 200 and 375 MHz transducers, respectively.

	Slope (10^{-3} dB/MHz)	y-intercept (dB)	MBF (dB)
Normal	-4.54 +/- 5.37	-19.25 +/- 1.31	-20.19 +/- 0.88
SMase	-32.10 +/- 13.47	-16.79 +/- 2.70	-23.41 +/- 1.85
Normal	-8.28 +/- 4.24	-16.81 +/- 1.99	-19.68 +/- 1.17
SMase	-72.34 +/- 29.48	-1.53 +/- 6.98	-26.20 +/- 3.79

For analysis of the spectral minima using the 900 MHz transducer, the normal RBCs showed no detectable minimum. In contrast, eryptotic RBCs had two minima detected within the transducer bandwidth. The two minima had mean frequencies of 641 ± 112 MHz and 1142 ± 93 MHz. The minima location is correlated to the apparent absorber size [15]. For normal RBCs the apparent size is the thickness of the center of the RBC (known to be approximately 0.75 µm). This results in a minimum outside the transducer bandwidth. However, eryptotic RBCs result in a shift of the minima to lower frequencies due to increase in its thickness. The size of each cell can be deduced by the location of the minima [20]. Assuming a spherical absorber, a first minimum of 641 MHz corresponds to a size of 1.61 µm [20]. From the optical images (Fig. 1) the size of RBCs induced with ceramide is more than 3 µm. The decrease in the measured apparent size from actual size of eryptotic RBC is due to the resolution volume of the 900 MHz ultrasound transducer, which is around 1.5 µm (see Fig. 5). Therefore, PA minima detection using a transducer with resolution smaller than the size of single RBC introduces a limitation due to the tight focusing of the transducer.

Fig. 3. Representative radiofrequency signals acquired using the PA microscope system with multiple ultrasound transducers. Top row represents signals from normal biconcave RBCs and bottom row represents signals from SMase exposed RBCs. Signals were acquired using transducers with center frequencies of 200, 375 and 900 MHz (left to right).

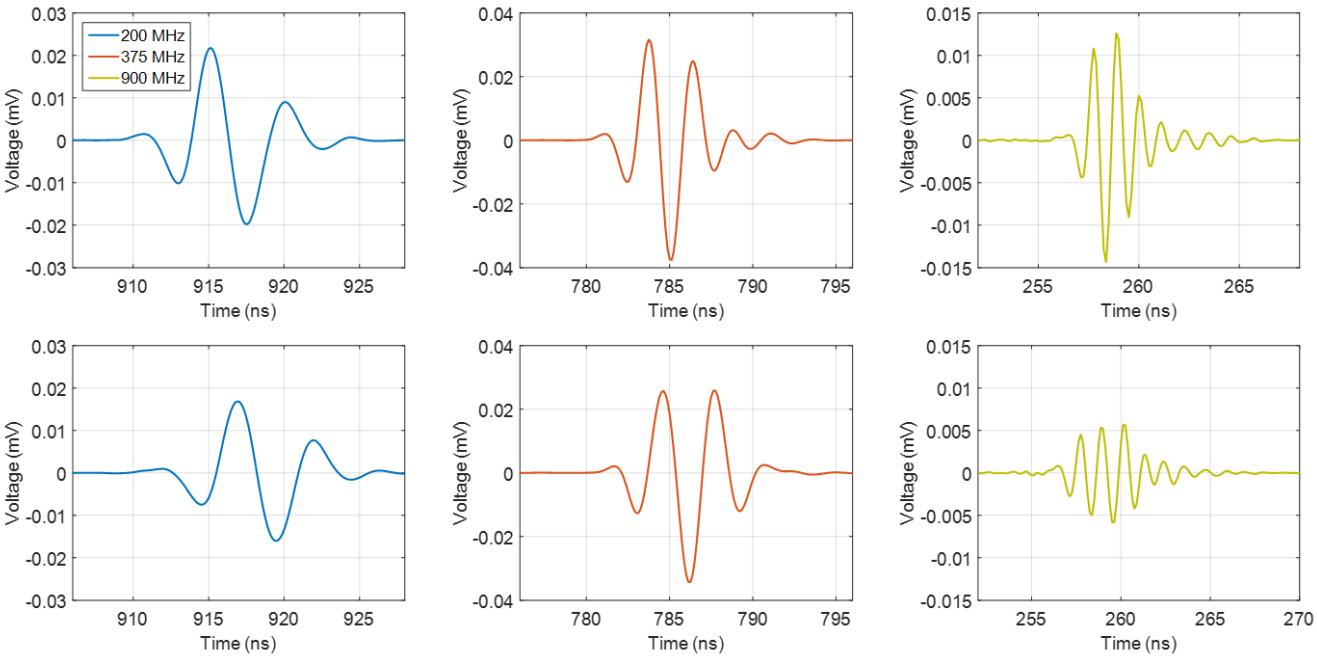

Fig. 4 Power spectra of normal biconcave RBCs (left) and SMase induced RBCs (right) acquired using three different ultrasound transducers with center frequencies of 200 (blue), 375 (red) and 900 (yellow) MHz.

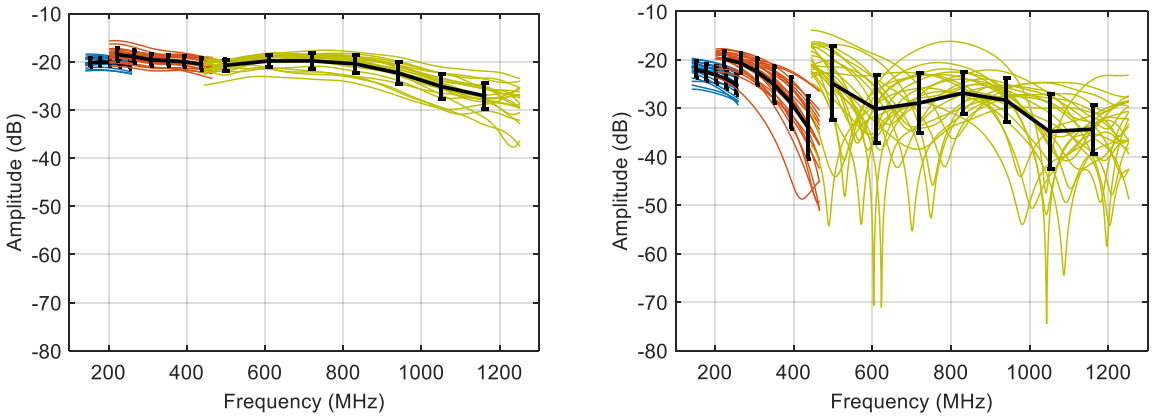

Fig. 5. Scalable images of the size of the RBCs and the focal spot (yellow) for 200, 375 and 900 MHz transducers for normal (top) and SMase (bottom) induced RBCs. The yellow shades represent the focal spot of the ultrasound transducers. In all cases, the laser was defocused to illuminate the entire RBC and is not shown in the figure.

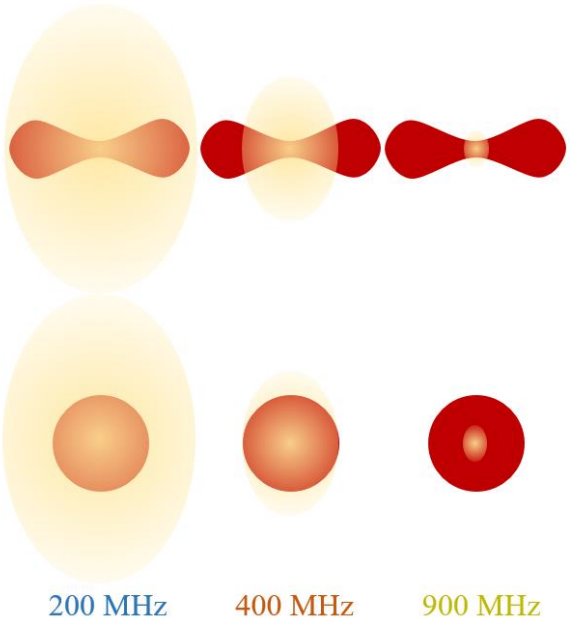

IV. Conclusion

Using PA spectral analysis, we were able to differentiate between biconcave RBCs and eryptotic RBCs at the single cell level using frequencies ranges between 150–1250 MHz. The results demonstrate an increase in the apparent thickness of eryptotic RBC through a decrease in the measured spectral slope. Also the results demonstrated the effect of ultrasound transducer on generated spectral parameters.

Acknowledgment

This project was funded by Natural Sciences and Engineering Research Council of Canada (NSERC) Postgraduate Scholarships (PGS) granted to Muhannad Fadhel. Terry Fox Foundation granted to Michael Kolios. Funding to purchase the equipment was provided by the Canada Foundation for Innovation (CFI) granted to Michael Kolios.

References

[1] B. Ogretmen and Y. A. Hannun, "Biologically active sphingolipids in cancer pathogenesis and treatment," *Nat. Rev. Cancer*, vol. 4, no. 8, pp. 604–616, Aug. 2004.

[2] B. Ogretmen, "Sphingolipids in cancer: Regulation of pathogenesis and therapy," *FEBS Lett.*, vol. 580, no. 23, pp. 5467–5476, Oct. 2006.

[3] P. E. Thorpe, "Vascular Targeting Agents as Cancer Therapeutics," *Clin. Cancer Res.*, vol. 10, no. 2, pp. 415–427, Jan. 2004.

[4] J. Folkman, P. Hahnfeldt, and L. Hlatky, "Cancer: looking outside the genome," *Nat. Rev. Mol. Cell Biol.*, vol. 1, no. 1, pp. 76–79, Oct. 2000.

[5] R. W. Jenkins, D. Canals, and Y. A. Hannun, "Roles and regulation of secretory and lysosomal acid sphingomyelinase," *Cell. Signal.*, vol. 21, no. 6, pp. 836–846, Jun. 2009.

[6] M. Garcia-Barros, F. Paris, C. Cordon-Cardo, D. Lyden, S. Rafii, A. Haimovitz-Friedman, Z. Fuks, and R. Kolesnick, "Tumor response to radiotherapy regulated by endothelial cell apoptosis," *Science*, vol. 300, no. 5622, pp. 1155–1159, May 2003.

[7] G. J. Czarnota, R. Karshafian, P. N. Burns, S. Wong, A. A. Mahrouki, J. W. Lee, A. Caissie, W. Tran, C. Kim, M. Furukawa, E. Wong, and A. Giles, "Tumor radiation response enhancement by acoustical stimulation of the vasculature," *Proc. Natl. Acad. Sci.*, vol. 109, no. 30, pp. E2033–E2041, Jul. 2012.

[8] S. Mallidi, G. P. Luke, and S. Emelianov, "Photoacoustic imaging in cancer detection, diagnosis, and treatment guidance," *Trends Biotechnol.*, vol. 29, no. 5, pp. 213–221, May 2011.

[9] A. Sadeghi-Naini, O. Falou, J. M. Hudson, C. Bailey, P. N. Burns, M. J. Yaffe, G. J. Stanisz, M. C. Kolios, and G. J. Czarnota, "Imaging innovations for cancer therapy response monitoring," *Imaging Med.*, vol. 4, no. 3, pp. 311–327, Jun. 2012.

[10] B. Zhao, L. H. Schwartz, and S. M. Larson, "Imaging surrogates of tumor response to therapy: anatomic and functional biomarkers," *J. Nucl. Med. Off. Publ. Soc. Nucl. Med.*, vol. 50, no. 2, pp. 239–249, Feb. 2009.

[11] S. Mallidi, G. P. Luke, and S. Emelianov, "Photoacoustic imaging in cancer detection, diagnosis, and treatment guidance," *Trends Biotechnol.*, vol. 29, no. 5, pp. 213–221, May 2011.

[12] S. Dinkla, K. Wessels, W. P. R. Verdurmen, C. Tomelleri, J. C. A. Cluitmans, J. Fransen, B. Fuchs, J. Schiller, I. Joosten, R. Brock, and G. J. C. G. M. Bosman, "Functional consequences of sphingomyelinase-induced changes in erythrocyte membrane structure," *Cell Death Dis.*, vol. 3, p. e410, 2012.

[13] F. Lang, E. Gulbins, P. A. Lang, D. Zappulla, and M. Föller, "Ceramide in suicidal death of erythrocytes," *Cell. Physiol. Biochem. Int. J. Exp. Cell. Physiol. Biochem. Pharmacol.*, vol. 26, no. 1, pp. 21–28, 2010.

[14] E. Lang, S. M. Qadri, and F. Lang, "Killing me softly - suicidal erythrocyte death," *Int. J. Biochem. Cell Biol.*, vol. 44, no. 8, pp. 1236–1243, Aug. 2012.

[15] E. M. Strohm, I. Gorelikov, N. Matsuura, and M. C. Kolios, "Modeling photoacoustic spectral features of micron-sized particles," *Phys. Med. Biol.*, vol. 59, no. 19, pp. 5795–5810, Oct. 2014.

[16] E. M. Strohm, E. S. L. Berndl, and M. C. Kolios, "Probing Red Blood Cell Morphology Using High-Frequency Photoacoustics," *Biophys. J.*, vol. 105, no. 1, pp. 59–67, Jul. 2013.

[17] E. M. Strohm and M. C. Kolios, "Sound velocity and attenuation measurements of perfluorocarbon liquids using photoacoustic methods," in *Ultrasonics Symposium (IUS), 2011 IEEE International*, 2011, pp. 2368–2371.

[18] J. C. Hansen, R. Skalak, S. Chien, and A. Hoger, "An elastic network model based on the structure of the red blood cell membrane skeleton.," *Biophys. J.*, vol. 70, no. 1, pp. 146–166, Jan. 1996.

[19] G. Xu, I. A. Dar, C. Tao, X. Liu, C. X. Deng, and X. Wang, "Photoacoustic spectrum analysis for microstructure characterization in biological tissue: A feasibility study," *Appl. Phys. Lett.*, vol. 101, no. 22, p. 221102, Nov. 2012.

[20] G. J. Diebold, M. I. Khan, and S. M. Park, "Photoacoustic 'signatures' of particulate matter: optical production of acoustic monopole radiation," *Science*, vol. 250, no. 4977, pp. 101–104, Oct. 1990.